Spatiotemporal chaos in rf-driven Josephson junction series arrays

Daniel Domínguez
Los Alamos National Laboratory, Theoretical Division, T-11, M.S. B262, Los Alamos, New Mexico 87545

Hilda A. Cerdeira
International Centre for Theoretical Physics, P. O. Box 586, Miramare, 34100 Trieste, Italy
(Received 20 December 1994; revised manuscript received 30 March 1995)

We study underdamped Josephson junction series arrays that are globally coupled through a resistive shunting load and driven by an rf bias current. They can be an experimental realization of many phenomena currently studied in globally coupled logistic maps. We study their spatiotemporal dynamics and we find coherent, ordered, partially ordered, turbulent, and quasiperiodic phases. The ordered phase corresponds to giant Shapiro steps in the IV characteristics. In the turbulent phase there is a saturation of the broad-band noise for a large number of junctions. This corresponds to a breakdown of the law of large numbers as seen in globally coupled maps. Coexisting with this phenomenon, we find an emergence of pseudosteps in the IV characteristics. This effect can be experimentally distinguished from the true Shapiro steps, which do not have broad-band noise emission. We study the stability of the breakdown of the law of large numbers against thermal fluctuations. We find that it is stable below a critical temperature T_{c1}. A measurement of the broad-band noise as a function of temperature T will show three different regimes: below T_{c1} the broad-band noise decreases when increasing T, and there is turbulence and the breakdown of the law of large numbers. Between T_{c1} and a second critical temperature T_{c2} the broad-band noise is constant and the dynamics is dominated by the chaos of the individual junctions. Finally above T_{c2} all the broad-band noise is due to thermal fluctuations, since it increases linearly with T.

I. INTRODUCTION

Josephson junction arrays are mesoscopic devices which can be fabricated with very specific properties and geometries.[1] In the last years they have become a good laboratory for the study of nonlinear dynamical systems with many degrees of freedom.[2–12] Moreover, they have potential applications as high frequency coherent power sources,[13,14] parametric amplifiers, and voltage standards.[13] One of the prototype models of nonlinear systems with many degrees of freedom is coupled logistic maps.[15] In particular, globally coupled maps (GCM's) have been studied as a mean-field-type extension of these models.[16,17] As a consequence of the interplay between temporal chaos and space synchronization, the GCM's exhibit coherent, ordered, partially ordered, and turbulent phases.[16] In the turbulent phase, a surprising result was found by Kaneko:[18] Even when spatial coherence is completely destroyed, a subtle collective behavior emerges. This was seen as a violation of the law of large numbers[18–24] as a function of the number of logistic maps.

We have made contact between these abstract models of GCM's and one-dimensional Josephson junction series arrays (JJSA's).[11,12] In this system, the role of the logistic maps is played by underdamped single Josephson junctions, which are known to show chaotic behavior when they are driven by a rf bias current.[25–28] The global coupling is achieved by connecting this junctions in series but with a common resistive shunting load. Therefore, the two conflicting trends of GCM are present: destruction of coherence due to the chaotic divergences of the individual junctions and synchronization through global averaging of the common shunting load. We have found[11] that the breakdown of the law of large numbers can be observed in rf-driven underdamped JJSA's, and that it is stable for temperatures below a certain T_{c1}.[12] Moreover, we find that whenever the JJSA shows a breakdown of the law of large numbers, pseudo Shapiro steps emerge in the IV characteristics of the JJSA.[11] This last effect is a result which does not result directly from previously known phenomena in GCM's. In this paper we discuss these phenomena in more detail, and we present a thorough analysis of the different dynamical regimes of the JJSA (not only the turbulent phase).

Josephson junction series arrays coupled by an external shunting load have been extensively studied before.[2–5] But in these studies the arrays were driven by a dc current. Since a single Josephson junction with a dc bias never shows chaos, the many interesting chaotic phenomena studied in Refs. 2–5 are a consequence of the high dimensionality of the system. On the other hand, the dynamics of rf-driven two-dimensional Josephson junction arrays has been of great interest in recent years, both experimentally[6] and theoretically.[7,8] Much of the interest has concentrated in the study of giant Shapiro steps and coherent vortex states. Some investigations of chaos and turbulence on two-dimensional Josephson junction arrays have also been done recently.[9,10] In particular Bhagavatula *et al.*[10] have studied chaos in two-dimensional rf-driven Josephson junction arrays. The main difference between the JJSA and the two-dimensional Josephson

0163-1829/95/52(1)/513(14)/$06.00

junction arrays simulated in Ref. 10 is that in the last case there is a locally coupled dynamics instead of the global coupling of the JJSA. Therefore, a breakdown of the law of large numbers is not likely to be found in their case.

The paper is organized as follows. In Sec. II we review the dynamics of chaos in a single Josephson junction, showing simulations for the parameters that will be used for the JJSA in the rest of the paper. In Sec. III we introduce the dynamical equations for the JJSA and compare them with the GCM dynamics. In Sec. IV we present a thorough study of the spatiotemporal dynamics of the JJSA for different coupling strengths and bias currents. In particular we identify the various dynamical phases and their consequences in the IV characteristics of the JJSA. In Sec. V we investigate the breakdown of the law of large numbers in the turbulent phase of the JJSA. In Sec. VI we discuss the effect of thermal noise on the turbulent phase of the JJSA. Finally in Sec. VII we present our conclusions and discuss possible experimental consequences of our findings.

II. CHAOS IN SINGLE JOSEPHSON JUNCTIONS

Before considering the JJSA, let us review the dynamics of a single Josephson junction. The supercurrent flowing through a Josephson junction is

$$I_J = I_c \sin\phi \ , \tag{1}$$

where ϕ is the phase difference of the complex order parameters in the two superconductors of the junction, and I_c is the maximum current that can flow through the junction. The voltage drop across the junction is

$$V = \frac{\hbar}{2e}\frac{d\phi}{dt} \ . \tag{2}$$

In real junctions one has to take into account that there is always a source of dissipation and that the junction also works as a capacitor. This is usually described with the resistively shunted junction (RSJ) model.[29] In a current-biased junction, the bias current $I(t)$ flows in parallel with an ideal Josephson junction, a resistor r, and a capacitor C so that the total current is given by

$$I(t) = I_J + \frac{V}{r} + C\frac{dV}{dt} = I_0 \sin\phi + \frac{\hbar}{2er}\frac{d\phi}{dt} + \frac{C\hbar}{2e}\frac{d^2\phi}{dt^2} \ . \tag{3}$$

It can be written in reduced units, with currents normalized by the critical current, $i = I/I_c$, voltages by rI_c, $v = V/rI_c$, and time normalized by the plasma frequency $\omega_p = \sqrt{\frac{2eI_c}{\hbar C}}$, $\omega_p t = \tau$, as

$$\ddot{\phi} + g\dot{\phi} + \sin\phi = i(\tau) \ , \tag{4}$$

where $g = (\frac{\hbar}{2eCr^2I_c})^{1/2} = 1/\beta_c^{1/2}$, with β_c the McCumber parameter.[29]

One of the responses that can be measured experimentally are the IV characteristics of the Josephson junctions, which is the time-averaged voltage $\langle v(\tau)\rangle = v$ as a function of the time-averaged bias current $\langle i(\tau)\rangle = i$. When the bias current $I(t)$ is time independent and the junction is overdamped ($C = 0$), Eq. (3) can be solved analytically.[30] In this case, the time-averaged voltage is $v = \sqrt{i^2 - 1}$ for $i > 1$ and $v = 0$ for $i < 1$.

When the junctions are rf biased, with $I(t) = I_{\rm dc} + I_{\rm rf}\sin(\omega_{rf}t)$, they show Shapiro steps.[31,30,25–28] These are plateaus in the IV characteristics where the voltages are quantized at

$$V_n = n\frac{\hbar\omega_{\rm rf}}{2e}, \quad n = 1, 2, 3, \dots \ , \tag{5}$$

or in reduced units $v = ng\Omega_{\rm rf}$, with $\Omega_{\rm rf} = \omega_{\rm rf}/\omega_p$. They correspond to phase-locked states, which are periodic solutions in resonance with the rf current, such that $\phi(\tau + 2\pi/\Omega_{\rm rf}) = \phi(\tau) + 2\pi n$. In the underdamped case $g < 1$, there are also subharmonic Shapiro steps for which $v = \frac{n}{m}g\Omega_{\rm rf}$. They correspond to periodic solutions of the type $\phi(\tau + 2\pi m/\Omega_{\rm rf}) = \phi(\tau) + 2\pi n$.

Chaotic behavior can occur in underdamped junctions ($g < 2$) driven by a rf current below the plasma frequency ($\Omega_{\rm rf} < 1$).[28] In these chaotic solutions the junction switches pseudorandomly between unstable, overlapping Shapiro steps.[25–28] It has also been shown that this dynamical system behaves as a circle map in certain cases.[26] Here, we study the chaotic nature of the solutions by computing the maximum Liapunov exponent λ of the dynamical system of Eq. (4). Experimentally,[27] most chaotic modes can be observed as broad-band noise in the power spectrum of the voltage. The power spectrum is computed as $S(\omega) = \frac{2}{t_m}|\int_0^{t_m} v(\tau)e^{i\omega\tau}d\tau|^2$. In the presence of broad-band noise, the low-frequency part of the spectrum approaches a constant, $S_0 = \lim_{\omega\to 0} S(\omega)$.

Let us study one example of Josephson junctions in which there are periodic solutions (Shapiro steps) and chaotic solutions. We choose a case with $g = 0.2$, $\Omega_{\rm rf} = 0.8$, and $i_{\rm rf} = 0.61$. We integrate the dynamical system of Eq. (4) using a fourth-order Runge-Kutta method with fixed step $\Delta\tau = T/160$, with $T = 2\pi/\Omega_{\rm rf}$ the period of the rf drive, and we iterate the dynamics for times as long as $1024T$, after discarding the first 256 periods. For some particular cases, we have checked our results with $\Delta\tau = T/320$ and integration time $2048T$.

In Fig. 1 we show the average voltage $v/g\Omega_{\rm rf}$, the Liapunov exponent λ, and the broad-band noise S_0 as a function of $i_{\rm dc}$. We distinguish four different regimes as a function of $i_{\rm dc}$. (i) There are periodic solutions, with $\lambda < 0$ and $S_0 \to 0$. They appear either below the critical current ($i_{\rm dc} < i_c = 0.036$), where there is no average dissipation $v = 0$, or at the Shapiro steps, which in this case are at voltages $\frac{1}{2}g\Omega_{\rm rf}$ ($0.256 < i_{\rm dc} < 0.428$) and $3g\Omega_{\rm rf}$ ($0.476 < i_{\rm dc} < 0.508$). (ii) There are chaotic solutions in the region between i_c and the step at $\frac{1}{2}g\Omega_{\rm rf}$ ($0.036 < i_{\rm dc} < 0.256$), for which $\lambda > 0$, S_0 finite. In this region some periodic "windows" are also seen (notably for voltages $\frac{1}{2}g\Omega_{\rm rf}$ and $\frac{1}{3}g\Omega_{\rm rf}$). (iii) For high currents ($i_{\rm dc} > 0.508$), where there is a linear resistive behavior

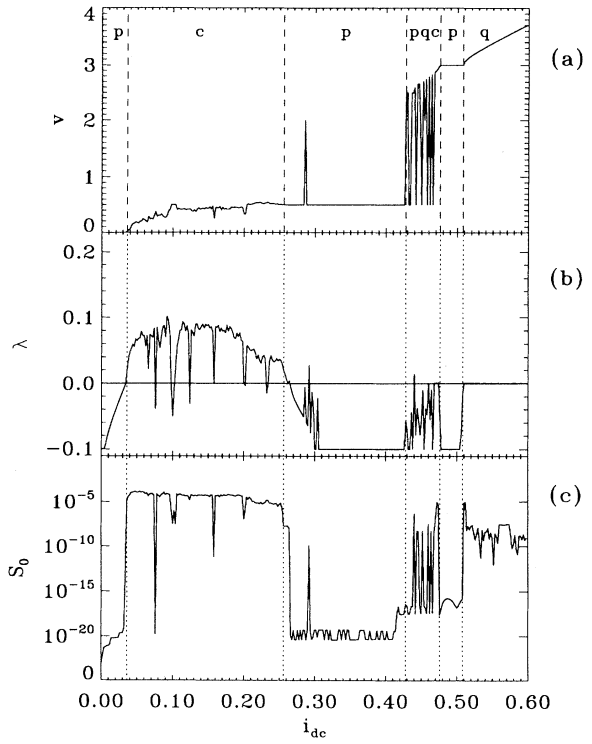

FIG. 1. (a) IV characteristics for one single Josephson junction with $g = 0.2$, $\Omega_{\rm rf} = 0.8$, $i_{\rm rf} = 0.61$. We have normalized the average voltage as $V = v/g\Omega_{\rm rf}$. (b) Maximum Liapunov exponent λ as a function of $i_{\rm dc}$. (c) Low frequency limit of the power spectrum S_0 as a function of $i_{\rm dc}$. Dynamical phases: p, mostly periodic solutions; q, mostly quasiperiodic solutions; c, mostly chaotic solutions.

in the IV characteristics, we find quasiperiodic solutions (also subharmonics with high m are possible here), for which $\lambda \approx 0$, S_0 small. (iv) Finally, between the two steps, there is a region ($0.428 < i_{\rm dc} < 0.476$) where either periodic solutions with $v = \frac{1}{2}g\Omega_{\rm rf}$, quasiperiodic solutions, or chaotic solutions can exist, depending on the initial conditions. In this region the IV characteristics show hysteresis. Note that we have deliberately chosen a case with few stable Shapiro steps. For this set of parameters, most of the Shapiro steps are unstable and overlapping, giving place to a wide region of chaotic states.

III. JOSEPHSON JUNCTION SERIES ARRAYS

A. Dynamical equations

Let us now consider an underdamped JJSA shunted by a resistive load,[2,32] and subjected to a *rf bias current* $I_B(t) = I_{\rm dc} + I_{\rm rf}\sin(\omega_{rf}t)$. This consists of a circuit where there are N junctions connected in series one after another, and there is a common resistive load in parallel to all the junctions (see Fig. 2). The dynamical behavior of each one of the Josephson junctions is described with the RSJ model of Eq. (3),

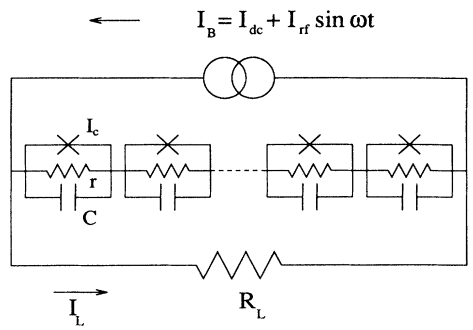

FIG. 2. Schematic circuit of a Josephson junction series array with a resistive load R_L and external current bias I_B. Each Josephson junction, with critical current I_c, is modeled including a shunt resistance r and a capacitance C.

$$I_c\sin\phi_k + \frac{\hbar}{2er}\frac{d\phi_k}{dt} + \frac{C\hbar}{2e}\frac{d^2\phi_k}{dt^2} = I_S \quad k = 1,\ldots,N\ , \tag{6}$$

where I_S is the current flowing through the circuit branch with the junctions in series. On the other hand, the common load satisfies

$$R_L I_L = \sum_{k=1}^{N} V_k = \sum_{k=1}^{N}\frac{\hbar}{2e}\frac{d\phi_k}{dt}\ , \tag{7}$$

where R_L is the resistance of the load and I_L is the current flowing through the load. The bias current divides between the load and the junctions in series,

$$I_B(t) = I_{\rm dc} + I_{\rm rf}\sin(\omega_{rf}t) = I_S + I_L\ . \tag{8}$$

Therefore, the governing equations of the JJSA in reduced units are

$$\ddot{\phi}_k + g\dot{\phi}_k + \sin\phi_k + \frac{\sigma}{N}\sum_{j=1}^{N} g\dot{\phi}_j = i_{\rm dc} + i_{\rm rf}\sin(\Omega_{\rm rf}\tau)\ , \tag{9}$$

where ϕ_k is the superconducting phase difference across the junction k and $k = 1,\ldots,N$. Here $\sigma = \frac{rN}{R_L}$ represents the strength of the global coupling in the array. Note that, when $\sigma = 0$, Eq. (9) reduces to a set of N independent junctions. Here, the voltage per junction $v(t) = \frac{1}{N}\sum_k v_k = \frac{1}{N}\sum_k g\dot{\phi}_k$ acts as a mean field variable.

B. Comparison with globally coupled logistic maps

One of the simplest models among globally coupled dynamical systems are the globally coupled maps (GCM's).[16] They were originally introduced as a mean field extension of coupled map lattices.[15] The GCM's are given by

$$x_{n+1}(i) = (1-\epsilon) f(x_n(i)) + \frac{\epsilon}{N} \sum_{j=1}^{N} f(x_n(j)), \qquad (10)$$

where $x_n(i)$ is a continuous variable $x(i)$ at *discrete* time n, with $i = 1, 2, \ldots, N$ labeling sites in a lattice, and ϵ is a measure of the coupling strength. The mapping function $f(x)$ is chosen such that it shows one-dimensional *chaos*. The simplest attractor of the GCM is the coherent attractor for which $x_n(i) = x_n$ for all i, and the system reduces to the single map $x_{n+1} = f(x_n)$. The most studied case is the well-known logistic map $f(x) = 1 - ax^2$. Also the same phenomena has been studied for the tent map,[16,18] $f(x) = a(\frac{1}{2} - |x - \frac{1}{2}|)$, and for globally coupled circle maps[17,3] as

$$x_{n+1}(i) = x_n + \frac{K}{2\pi} \sin[2\pi x_n(i)] + \Omega + \frac{\epsilon}{2\pi N} \sum_j \sin[2\pi x_n(j)]. \qquad (11)$$

The main ingredients of GCM's are that (i) the individual elements are chaotic and (ii) there is an additive coupling with the same weight for all the elements. The first condition means that the GCM is reduced to a chaotic one-dimensional system either for $N = 1$ (single map) or for $\epsilon = 0$ (ensemble of uncoupled maps), which coincides with the coherent attractor, $x_{n+1} = f(x_n)$. As a consequence, the system has two conflicting tendencies, random behavior and incoherence because of the chaotic instabilities of the single elements, and synchronization because of global averaging by the coupling term.

The JJSA studied here satisfies both conditions. To make the analogy more obvious, the dynamical equations (9) can be rewritten as

$$\ddot{\phi}_k + (\tilde{g} - \epsilon)\dot{\phi}_k + \sin\phi_k + \frac{\epsilon}{N} \sum_{j=1}^{N} \dot{\phi}_j = i_{\rm dc} + i_{\rm rf} \sin(\Omega_{\rm rf}\tau) , \qquad (12)$$

with $\tilde{g} = (1+\sigma)g$ and $\epsilon = \sigma g$. Either in the limit $\epsilon = 0$ or $N = 1$, it reduces to

$$\ddot{\phi}_0 + \tilde{g}\dot{\phi}_0 + \sin\phi_0 = i_{\rm dc} + i_{\rm rf} \sin(\Omega_{\rm rf}\tau) , \qquad (13)$$

which is also the coherent attractor of the JJSA, $\phi_k(t) = \phi_0(t)$. This corresponds to the dynamics of a single Josephson junction as given by Eq. (4). As discussed in Sec. II in the underdamped case and with a rf bias it can have chaotic behavior. Therefore, the only difference with GCM's is that in the JJSA the time is a continuous variable and the dynamics is governed by differential equations instead of maps. Note that previously studied JJSA's (Refs. 2–5) do not follow condition (i). They have been studied only for dc current bias ($i_{\rm rf} = 0$), in which case the single-junction equation does not have chaos. Therefore, their dynamics can not be compared directly with GCM's. In this case the many interesting chaotic phenomena observed arise only from the high dimensionality of the system.

A closely related system is globally coupled oscillators (GCO's).[33,34] They are described by equations like

$$\dot{\phi}_i = \omega + g\frac{1}{N} \sum_{j=1}^{N} \Gamma(\phi_i - \phi_j) , \qquad (14)$$

where ϕ_i is a phase, and the coupling Γ is 2π periodic. These systems have a continuous time and in that sense they are similar to the JJSA. In the absence of coupling, $g = 0$, each unit is moving around its limit cycle at frequency ω. The GCO's are, therefore, similar to the JJSA with a dc current bias only,[2–4] for large currents $I_{dc} \gg I_0$ in the overdamped limit. This is because in that case the single-junction dynamics reduces to the limit cycle $\dot{\phi} = \omega \approx 2erI_{\rm dc}/\hbar$.

An important concept in both GCM's and GCO's is "clustering".[16,33] This means that even when all the elements (i.e., the junctions in the JJSA) are identical, the dynamics can break into different clusters, each of which consists of fully synchronized elements. After the system has fallen in an attractor, we say that i, j are in the same cluster if $x_n(i) = x_n(j)$. An attractor can be characterized by the number of clusters it has, $n_{\rm cl}$, and the number of elements of each cluster $(M_1, M_2, \ldots, M_{n_{\rm cl}})$. Four types of attractors have been identified in GCM's:[16] (i) the coherent attractor $n_{\rm cl} = 1$; (ii) attractors with few clusters, $n_{\rm cl} \ll N$; (iii) attractors with a large number of clusters, $n_{\rm cl} \sim N$, and large M_1 [for example, $n_{\rm cl} = N/2 + 1, (N/2, 1, 1, \ldots, 1)$]; (iv) attractors with a large number of clusters, $n_{\rm cl} \sim N$ and all M_j small ($M_j \sim 1, 2$). We will use this concept of clustering in the next section in our study of the dynamical regimes of the JJSA.

IV. SPATIOTEMPORAL CHAOS AND *IV* CHARACTERISTICS

Let us study the spatiotemporal behavior of the JJSA for different values of $i_{\rm dc}$ and σ. To compare with the single-junction case presented in Sec. II, we choose $\tilde{g} = 0.2$, $\Omega_{\rm rf} = 0.8$, and $i_{\rm rf} = 0.61$. We work with fixed $\tilde{g}$, instead of g, in order to have in all the cases the same coherent attractor. We integrate the dynamical system of Eq. (9) with the same numerical procedure as in the previous section. For each run we used different sets of random initial conditions $\{\phi_k(0), \dot{\phi}_k(0)\}$.

In Figs. 3, 4, and 5 we show our results for different values of the coupling, $\sigma = 0.05$, $\sigma = 0.2$, and $\sigma = 0.8$, respectively, and fixed size $N = 128$. First, we plot the *IV* characteristics, i.e., the average voltage per junction, $v = \frac{1}{N}\sum_j \langle g\dot{\phi}_j \rangle$, vs the dc bias $i_{\rm dc}$, in Figs. 3(a), 4(a), and 5(a). Note that v, which is the quantity that can be measured directly in the experiments, is also the time average of the "mean field," $v(\tau) = \frac{1}{N}\sum_j g\dot{\phi}_j$, in the globally coupled dynamical equations. At the same time, we analyze the spatiotemporal behavior of the solutions for each bias $i_{\rm dc}$. In what regards the temporal behavior, we plot the maximum Liapunov exponent λ of the system in Figs. 3(b), 4(b), and 5(b). In what regards the spatial behavior, we plot the number of clusters, $n_{\rm cl}$ in Figs. 3(c),

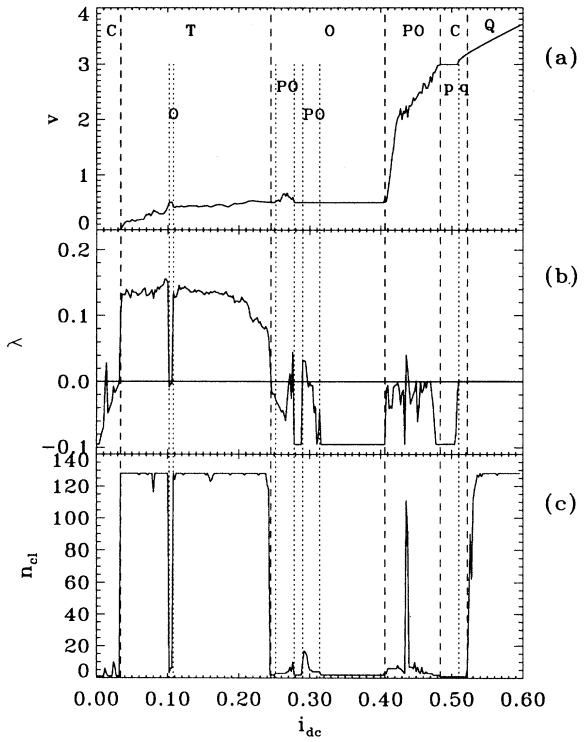

FIG. 3. (a) *IV* characteristics for a Josephson junction series array with $\tilde{g} = 0.2$, $\Omega_{rf} = 0.8$, $i_{rf} = 0.61$, $N = 128$ junctions, and coupling $\sigma = 0.05$. The average voltage per junction is normalized as $V = \bar{v}/g\Omega_{rf}$. (b) Maximum Liapunov exponent λ as a function of i_{dc}. (c) Number of clusters n_{cl} as a function of i_{dc}. C, coherent phase, which can have either periodic (p) or quasiperiodic (q) solutions; O, ordered phase; PO, partially ordered phase; T, turbulent phase; Q, quasiperiodic phase.

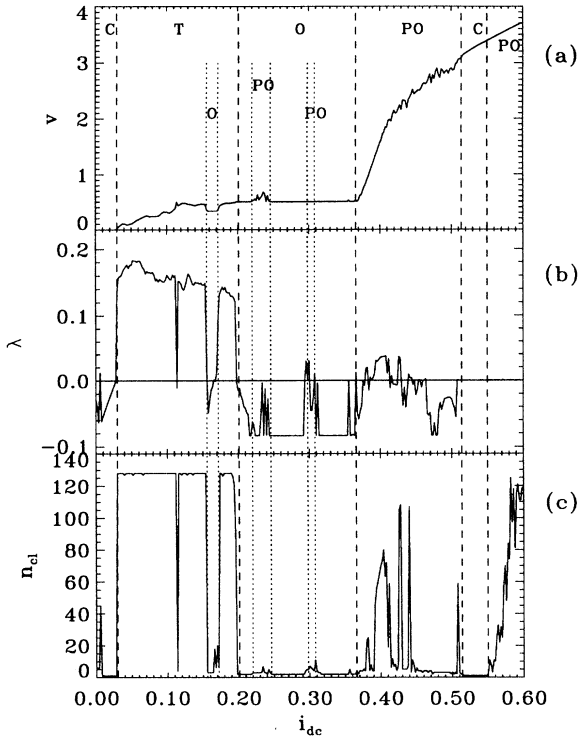

FIG. 4. The same as in Fig. 3 but for coupling $\sigma = 0.2$.

4(c), and 5(c). The criterion for clustering is that two sites i, j belong to the same cluster if $\phi_i = \phi_j + 2\pi n$, with n an integer. We find five different phases.

(a) *Turbulent phase*: all the attractors have many clusters, $n_{cl} \sim N$, and their temporal behavior is chaotic $\lambda > 0$. An example of this case is shown in Fig. 6(a). There we plot the time evolution for each site, showing the points in time where each phase ϕ_j hits $2\pi n$. We see that all the junctions follow a different time evolution, and none of them is periodic. The chaotic behavior is also evident in the power spectrum of the voltage $v(\tau)$ shown in Fig. 7(a). Besides the peaks corresponding to the driving frequency ω_{rf}, the spectrum is broad and tends to a constant at zero frequency. The turbulent phase appears always between the critical current i_c and the 1/2-integer Shapiro step in the *IV* characteristics, for this choice of parameters. Also for high values of σ it can be found at higher bias currents (see Fig. 5).

(b) *Ordered phase*: the attractors have few clusters, and they are periodic in time. This phase corresponds to Shapiro steps in the *IV* characteristics. In Fig. 6(b) we show an example for a 1/3-integer Shapiro step

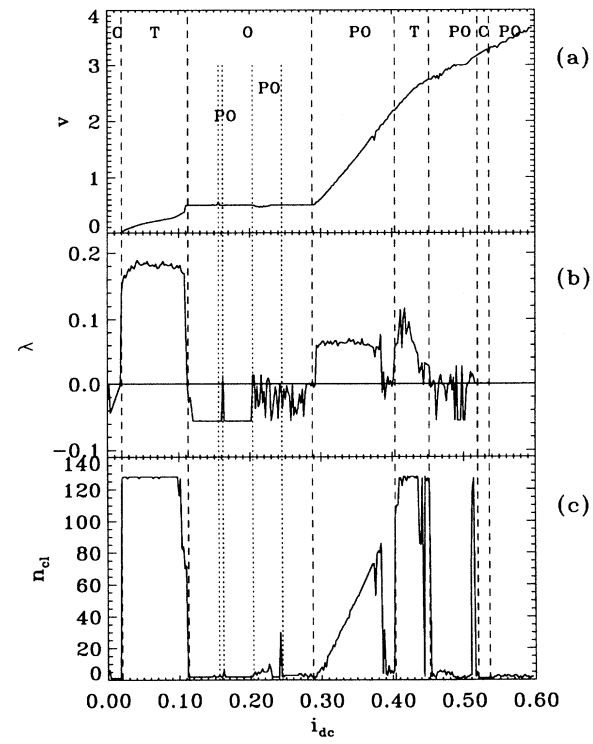

FIG. 5. The same as in Fig. 3 but for coupling $\sigma = 0.8$.

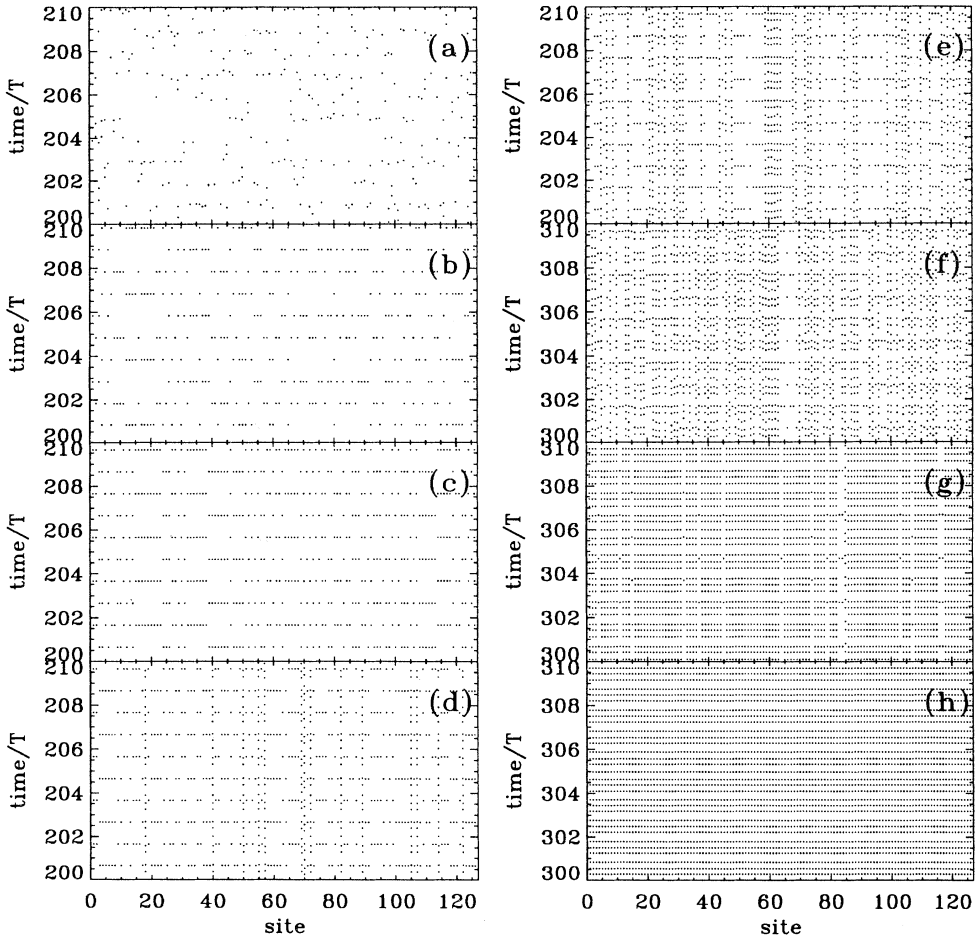

FIG. 6. Spatiotemporal evolution diagrams. For a system with $\tilde{g} = 0.2$, $\Omega_{\rm rf} = 0.8$, $i_{\rm rf} = 0.61$, $N = 128$ junctions, and coupling $\sigma = 0.2$. Each point represents the time when each junction phase ϕ_k hits $2n\pi$. (a) For a turbulent state, $i_{\rm dc} = 0.084$. For ordered states: (b) $i_{\rm dc} = 0.160$, 1/3-integer Shapiro step; (c) $i_{\rm dc} = 0.280$, 1/2-integer Shapiro step. For partially ordered states, (d) $i_{\rm dc} = 0.378$, (e) $i_{\rm dc} = 0.390$, (f) $i_{\rm dc} = 0.404$, (g) $i_{\rm dc} = 0.460$. (h) For a coherent state, $i_{\rm dc} = 0.520$.

($v/g = \frac{1}{3}\Omega_{\rm rf}$). We see that there are $n_{\rm cl} = 3$ clusters evenly distributed, each cluster oscillating with period $3T$ ($T = 2\pi/\omega_{\rm rf}$). This is also evident in the power spectrum shown in Fig. 7(b), where there are subharmonic peaks at frequencies $\omega = \frac{n}{3}\omega_{\rm rf}$. Another example, corresponding to a 1/2-integer Shapiro step ($v/g = \frac{1}{2}\Omega_{\rm rf}$), is shown in Fig. 6(c) and its corresponding power spectrum in Fig. 7(c). In this case there are $n_{\rm cl} = 2$ clusters, each one of them oscillating with period $2T$. Therefore there are subharmonic peaks in the power spectrum at frequencies $\omega = \frac{n}{2}\omega_{\rm rf}$. We always find that for p/q-integer Shapiro steps ($v/g = \frac{p}{q}\Omega_{\rm rf}$) there are $n_{\rm cl} = q$ clusters with period qT. In particular, for the case of integer steps ($q = 1$), they fall in a coherent attractor (for example, in Fig. 3 for $\sigma = 0.05$ in the step at $v/g = 3\Omega_{\rm rf}$). We mention that similar periodic attractors with a small number of clusters have also been found in globally coupled oscillator systems.[33,34]

(c) *Partially ordered phase*: depending on the initial conditions, there are attractors with few clusters or with many clusters unevenly distributed [type (iii) attractor in Sec. III(b)]. Let us discuss some examples. In Fig. 6(d) we show a case with $n_{\rm cl} = 4$ clusters and $M_i = (77, 34, 12, 5)$, which is temporally periodic since $\lambda < 0$. Two of the clusters ($M_1 = 77, M_2 = 34$) are in a periodic state with $v/g = \frac{1}{2}\Omega_{\rm rf}$ and the other two ($M_3 = 12, M_4 = 5$) in a periodic state with $v/g = 2.5\Omega_{\rm rf}$. The power spectrum in Fig. 7(d) shows subharmonic peaks. Another case is shown in Fig. 6(e), with $n_{\rm cl} = 4$ clusters but temporally chaotic $\lambda > 0$. There are two periodic clusters that correspond to $v/g = \frac{1}{2}\Omega_{\rm rf}$, and the other two are chaotic. The corresponding power spectrum in Fig. 7(e) shows both subharmonic peaks and broad-band noise. In Fig. 6(f) we show a case with $n_{\rm cl} = 80$ clusters ($n_{\rm cl} \sim N = 128$), which is temporally chaotic ($\lambda > 0$). The clusters are unevenly distributed $M_i = (26, 24, 1, 1, 1, \ldots, 1)$. The first two large clusters correspond to a periodic solution with $v/g = \frac{1}{2}\Omega_{\rm rf}$, whereas the other 78 single clusters are chaotic, but with average voltage $v/g \approx 2.5\Omega_{\rm rf}$. The last example of this phase is shown in Fig. 6(g). There are $n_{\rm cl} = 4$ clusters unevenly distributed $M_i = (114, 10, 3, 1)$ and the maximum Liapunov exponent is $\lambda \approx 0$. The large cluster $M_1 = 114$ corresponds to a quasiperiodic solution, and the small clusters correspond to periodic solutions with $v/g = \frac{1}{2}\Omega_{\rm rf}$ and with $v/g = 2\Omega_{\rm rf}$. Their power spectrum, shown in Fig. 7(g), has both subharmonic peaks and quasiperiodic peaks at incommensurate frequencies. We found the partially ordered phase with all this different type of solutions mostly at large currents above the big 1/2-integer Shapiro step, for this case.

(d) *Coherent phase*: here all the junctions oscillate

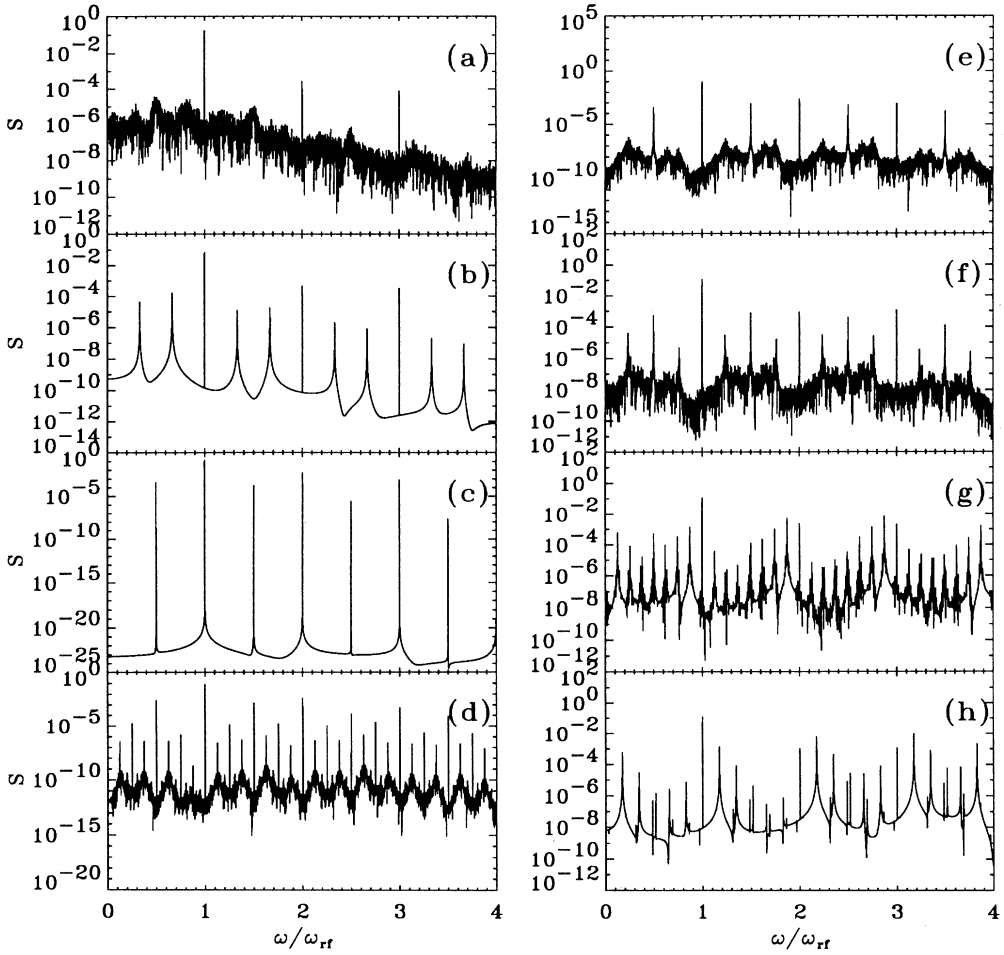

FIG. 7. Power spectra $S(\omega)$ of the voltage $v(\tau)$. For a system with $\tilde{g} = 0.2$, $\Omega_{rf} = 0.8$, $i_{rf} = 0.61$, $N = 128$ junctions, and coupling $\sigma = 0.2$. (a) For a turbulent state, $i_{dc} = 0.084$. For ordered states: (b) $i_{dc} = 0.160$, 1/3-integer Shapiro step; (c) $i_{dc} = 0.280$, 1/2-integer Shapiro step. For partially ordered states, (d) $i_{dc} = 0.378$, (e) $i_{dc} = 0.390$, (f) $i_{dc} = 0.404$, (g) $i_{dc} = 0.460$. (h) For a coherent state, $i_{dc} = 0.520$.

with the same phase, $n_{cl} = 1$. It occurs for periodic solutions either below the critical current ($v = 0$) or at integer Shapiro steps ($v/g = n\Omega_{rf}$) and for quasiperiodic solutions at large currents. This last case is shown in Fig. 6(h), and its corresponding power spectrum in Fig. 7(h), where there are peaks at incommensurate frequencies.

(e) *Quasiperiodic phase*: the attractors have a large number of clusters, $n_{cl} \sim N$, but their behavior is quasiperiodic in time ($\lambda \sim 0$). This phase appears at very large currents, when the IV curve is practically linear. A similar phase has been found in globally coupled circle maps[17] (but not in logistic GCM's). It has been suggested[17] to correspond to the phenomena of "attractor crowding".[3]

We have calculated the probability distribution in time of the phases in a fixed site j. This is the probability $P_t(\phi_j^{(n)})$ with $\phi_j^{(n)} = \phi_j(t_0 + nT)$ for fixed j and all the realizations of n. This is shown in Fig. 8(a). Since we calculate the probability only every period of the rf bias, the periodic attractors with period qT show q peaks in P_t, and the chaotic and quasiperiodic states show a broad distribution. Also in Fig. 8(b) we have calculated the probability distribution in space $P_s(\phi_j(t))$ for a given time t. Therefore, a distribution P_s with a few peaks corresponds to an attractor with n_{cl} = number of peaks, whereas a broad distribution corresponds to a turbulent attractor. Both plots correspond to $\sigma = 0.2$ and show the distributions as a function of i_{dc}. We see that the main qualitative difference in the temporal and spatial distributions is in the partially ordered phase. In the ordered phase both have the same peaks (periodicity=number of clusters), and in the turbulent phase both have broad distributions (but they do not coincide).

Finally, in Fig. 9 we show a complete phase diagram in the σ vs i_{dc} plane. We see that in general the tendency for increasing σ is that the turbulent phase reduces in size, the ordered phase (1/2-integer Shapiro step) displaces to lower i_{dc} values, and the partially ordered phase grows in size. For large σ a new turbulent phase develops in the middle of the partially ordered phase. We do not find that, as in GCM's, the coherent phase is the dominant attractor in the large coupling limit. Instead, there is always a rich structure with all the five phases present.

V. BREAKDOWN OF THE LAW OF LARGE NUMBERS AND PSEUDOSTEPS

Let us now study the turbulent phase in detail. As discussed in the previous section, in this phase the time evolution is chaotic ($\lambda > 0$) and practically all the junc-

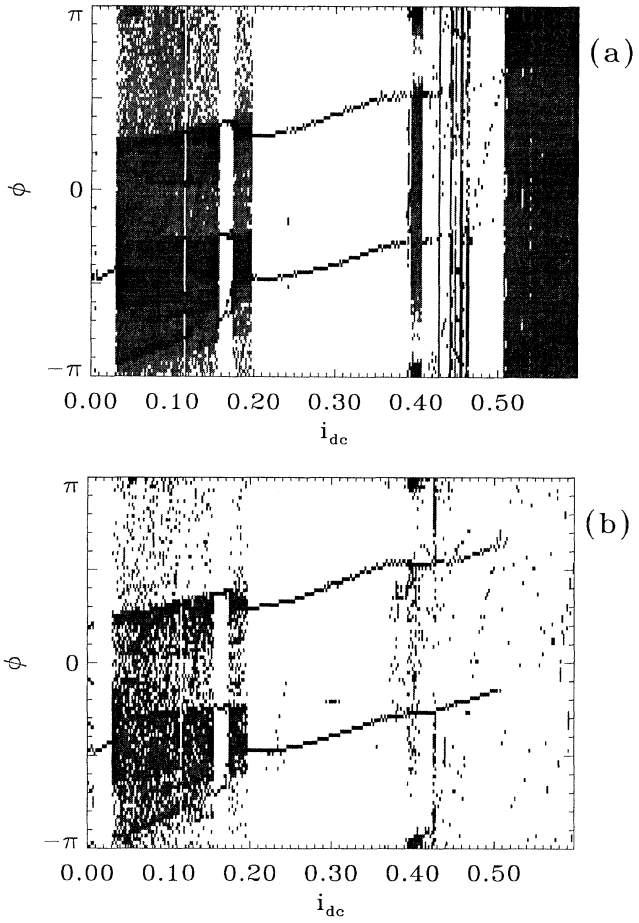

FIG. 8. Probability distribution of phases $\phi_k(t)$ as a function of $i_{\rm dc}$. For $\tilde{g} = 0.2$, $\Omega_{\rm rf} = 0.8$, $i_{\rm rf} = 0.61$, $N = 128$ junctions, and coupling $\sigma = 0.2$. (a) Temporal behavior: distribution for a given junction k as a function of time. (b) Spatial behavior: distribution of phases at a given time t. Grey scale: white $\equiv P(\phi) = 0$, black $\equiv P(\phi) = 1$.

tions have different phases ($n_{cl} \sim N$). Some interesting properties arise when studying the system as a function of the number of junctions.

First, let us see how the chaos depends on N. In Fig. 10 we plot the maximum Liapunov exponent as a function of N for different values of σ, for a given bias in the turbulent phase ($i_{\rm dc} = 0.124$). We see that λ grows with N and seems to saturate in limit $N \to \infty$. In a system with local coupling, like coupled map lattices, it is always possible to define a characteristic length scale ξ in the behavior of $\lambda(N)$ in the "turbulent" regimes.[15] But in our case there is no characteristic scale in Fig. 10 since, because of the global coupling, all the elements are equally close in distance (i.e., it is equivalent to an infinite-dimensional lattice).

Instead of λ, another quantity that has been studied in GCM's is the fluctuations of the mean field.[18–24] For example, in the GCM of Eq. (10) the mean field is $h_n = (1/N)\sum_i f(x_n(i))$. Kaneko[18] studied the mean square deviations of the mean field $\langle(\delta h)^2\rangle = \langle(h - \langle h\rangle)^2\rangle$, with $\langle\cdots\rangle$ the average over time and initial conditions. In the turbulent phase each element $x(i)$ is chaotic and different for each i. If they can be taken as random uncorrelated numbers, then the mean field fluctuations would follow the law of large numbers, $\langle(\delta h)^2\rangle \propto 1/N$. Thus in the thermodynamic limit $N \to \infty$ the GCM could be reduced to N independent logistic maps. However, Kaneko[18] found that the law of large numbers is broken in GCM's, and $\langle(\delta h)^2\rangle$ tends to a constant for large N. The existence of this size-independent fluctuation suggests that there is a remaining correlation between elements. This means that in the turbulent phase the different variables are not independent even in the thermodynamic limit. This dependence has been quantified by Kaneko by measuring the mutual information between elements.[18] It was found that there remains a finite mutual correlation even in the $N \to \infty$ limit. This question of the relation between synchronization and chaotic be-

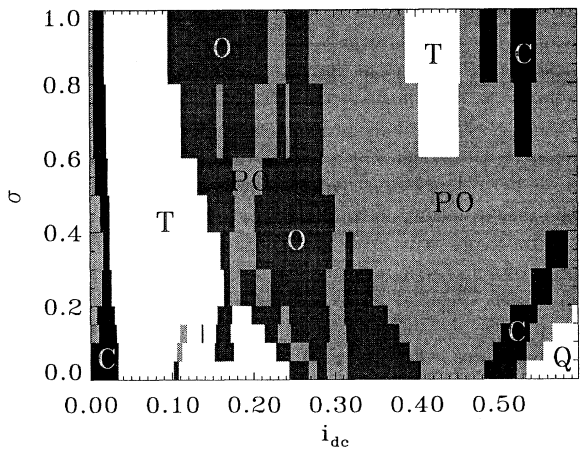

FIG. 9. Phase diagram in the σ vs $i_{\rm dc}$ plane. For a Josephson junction array with $\tilde{g} = 0.2$, $\Omega_{\rm rf} = 0.8$, $i_{\rm rf} = 0.61$, $N = 128$ junctions. C, coherent phase; O, ordered phase; PO, partially ordered phase; T, turbulent phase; Q, quasiperiodic phase.

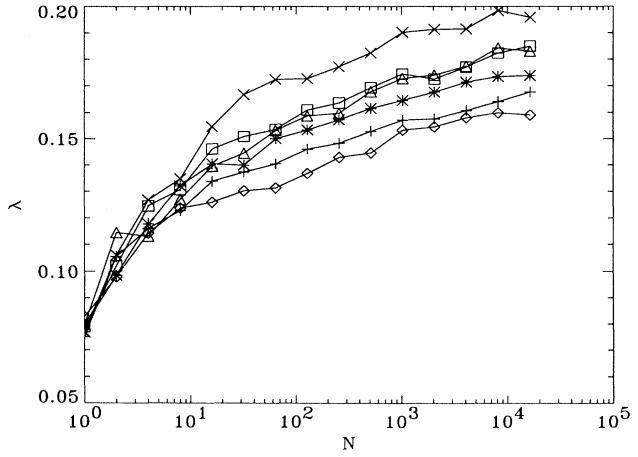

FIG. 10. Maximum Liapunov exponent λ in the turbulent phase as a function of the number N of junctions. For $\tilde{g} = 0.2$, $\Omega_{\rm rf} = 0.8$, $i_{\rm rf} = 0.61$, fixed bias $i_{\rm dc} = 0.124$, and different couplings: +, $\sigma = 0.1$; $*$, $\sigma = 0.15$; $\diamond$, $\sigma = 0.2$; $\triangle$, $\sigma = 0.3$; $\square$, $\sigma = 0.4$; $\times$, $\sigma = 0.5$.

havior has been an important topic in the framework of neuronal modeling; see Ref. 35. In the GCM this mutual correlation has been interpreted as a hidden coherence in the turbulent phase. This coherence shows, for example, in an emergence of broad peaks in the power spectrum of h_n.[18,19] However, an understanding of the origin of this hidden coherence and the frequency dependence of these broad peaks is still lacking in this problem. One of the intriguing questions is that a GCM of tent maps does follow the $1/N$ law.[18,23,24] Since the tent map does not have periodic windows, it is believed that the periodic windows may be relevant in the origin of the breakdown of the law of large number and emergence of peaks in the power spectrum.[18,19,23,24] These and related questions have motivated some discussion in the literature very recently.[21–24]

Regardless of the origin of the breakdown of the law of large numbers in GCM's, we study here this phenomenon in JJSA's, since it may lead to some experimental consequence in this system. First of all, let us note that in this case the voltage per junction, $v^{(N)}(t) = \frac{1}{N}\sum_{j=1}^{N} g\dot{\phi}_j$, acts as the "mean field" in Eq. (9). Since in the turbulent phase the $\phi_j(t)$ and, therefore, the $\dot{\phi}_j(t)$ are chaotic and different for different j, the fluctuations of $v(t)$ are the quantity that interests us here. However, since this is a periodically driven system, $\langle(\delta v)^2\rangle = \langle(v - \langle v\rangle)^2\rangle$ will not only be due to noisy fluctuations but also to the amplitude of the rf-induced oscillations in $v(t)$. [Even in the Shapiro steps it is $\langle(\delta v)^2\rangle \neq 0$.] Instead, we have to study the power spectrum of $v(t)$ which can be written as

$$S(\omega) = \frac{1}{N}|v_j(\omega)|^2 + \frac{1}{N^2}\left[\sum_{i\neq j} v_i(\omega)v_j^*(\omega)\right] , \qquad (15)$$

with $v_j(\omega)$ the Fourier transform of $v_j(t) = g\dot{\phi}_j(t)$. If the $\dot{\phi}_j(t)$ are completely independent, the second term in (15) will vanish for low frequencies, $\omega \to 0$. Therefore $S_0^{(N)} \sim \frac{1}{N}S_0^{(1)}$, with $S_0^{(N)}$ the low-frequency part of the power spectrum of a JJSA with N junctions. This is the equivalent of the law of large numbers for a periodically driven system. If it were valid, we could expect that in the large N limit the broad band noise part of $v^{(N)}(t)$ will tend to vanish ($S_0 \to 0$, for $N \to \infty$), reducing the dynamics of the JJSA to N independent chaotic junctions with an additional time-periodic driving $C(t) = v^{(N\to\infty)}(t)$. On the other hand, a finite value in the limit $S_0(N \to \infty)$ will be a measure of the strength of the remaining synchrony between junctions in the turbulent regime, coming from the second term in Eq. (15).

In Fig. 11 we show the calculated values of S_0 as a function of N for different values of σ and for $i_{dc} = 0.124$ (similar behavior is also seen for other values of i_{dc} within the turbulent phase). We see that for some values of the coupling σ, S_0 does not follow the law of large numbers since it saturates for large N. However, for $\sigma > 0.5$ or for

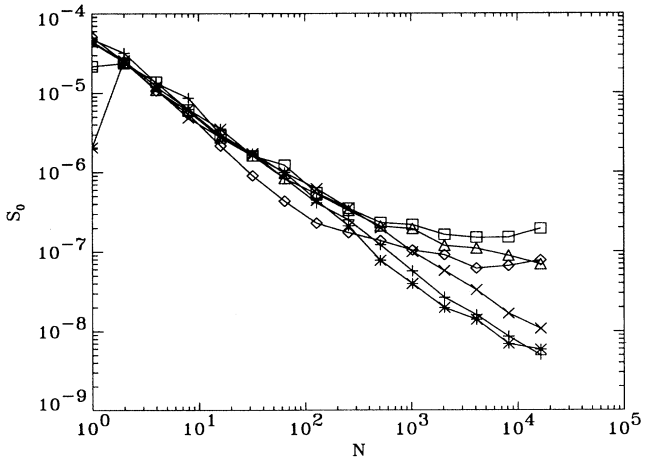

FIG. 11. Low-frequency limit of the power spectrum, $S_0 = \lim_{\omega\to 0} S(\omega)$, as a function of the number N of junctions. For $\tilde{g} = 0.2$, $\Omega_{rf} = 0.8$, $i_{rf} = 0.61$, $i_{dc} = 0.124$, and different values of the coupling: +, $\sigma = 0.1$; *, $\sigma = 0.15$; ◇, $\sigma = 0.2$; △, $\sigma = 0.3$; □, $\sigma = 0.4$; ×, $\sigma = 0.5$.

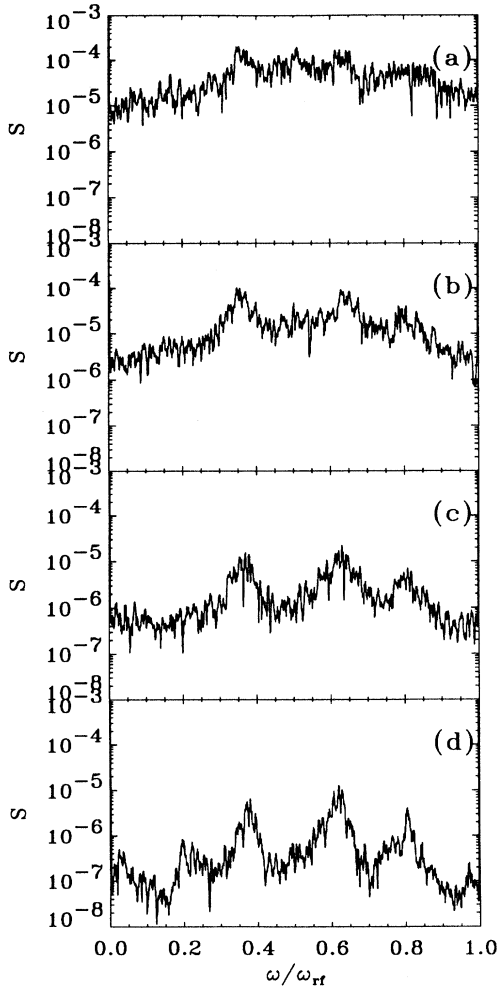

FIG. 12. Power spectrum of $v(\tau)$ for a turbulent state, with increasing N. For $\tilde{g} = 0.2$, $\Omega_{rf} = 0.8$, $i_{rf} = 0.61$, $i_{dc} = 0.124$, and $\sigma = 0.4$. (a) $N = 4$. (b) $N = 16$. (c) $N = 128$. (d) $N = 16\,384$.

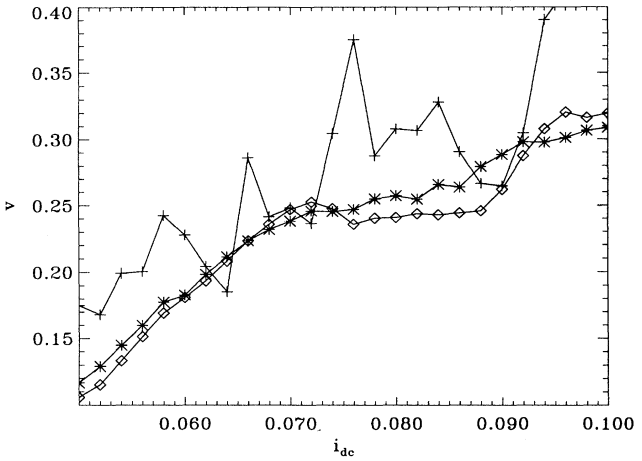

FIG. 13. Detailed IV curve in the turbulent phase, showing the emergence of a pseudostep when increasing N. For $\tilde{g} = 0.2$, $\Omega_{rf} = 0.8$, $i_{rf} = 0.61$, and $\sigma = 0.4$. (+, $N = 1$; $*$, $N = 16$; $\diamond$, $N = 128$).

$\sigma < 0.1$ we find that it follows the $1/N$ law for the values of N we can simulate. Therefore, this phenomenon seems to happen only for intermediate coupling σ in the JJSA.

We also studied the full power spectrum $S(\omega)$ in the turbulent phase. In Fig. 12 we show the low-frequency part of the spectra, $\omega < \Omega_{rf}$, for increasing number of junctions, for a case that has a breakdown of the law of large numbers. We see that for small N the power spectrum is flat. But when N increases it develops broad peaks. They get sharper with increasing N, up to when S_0 saturates, and then for higher values of N the spectrum remains invariant. This is the same kind of hidden coherence that has been found in GCM's (Refs. 18 and 19) as we mentioned previously.

We find that this subtle coherence of the turbulent phase notably affects the IV characteristics of the JJSA. We find that "pseudosteps" emerge in the IV curve for large N at the same time that S_0 saturates in the turbulent phase. This can be seen in Fig. 13. There we see that, while for $N = 1$ the IV curve in this region has a "noisy" aspect, when increasing N a plateau or pseudostep tends to appear. Many pseudosteps are present all along the range of i_{dc} corresponding to the turbulent phase for the various values of σ for which there is a breakdown of the law of large number, as we show in Fig. 14. Note that $N = 128$ is a value before the full saturation of S_0, since it is hard to simulate very large N for the full IV characteristics. However, we see that the pseudosteps emerge and sharpen up with increasing N, always in coexistence with a saturation of S_0. These pseudosteps are not true Shapiro steps, since they do not correspond to mode-locked periodic states. Instead, they have a positive Liapunov exponent and finite broad-band noise emission. This emergence of pseudosteps within the turbulent regime of the JJSA is a new result which one could not have predicted from our previous knowledge of GCM's. They seem to arise as an additional effect originated by the fact that we have a system of coupled nonlinear differential equations with a time-periodic drive, instead of simply coupled logistic maps.

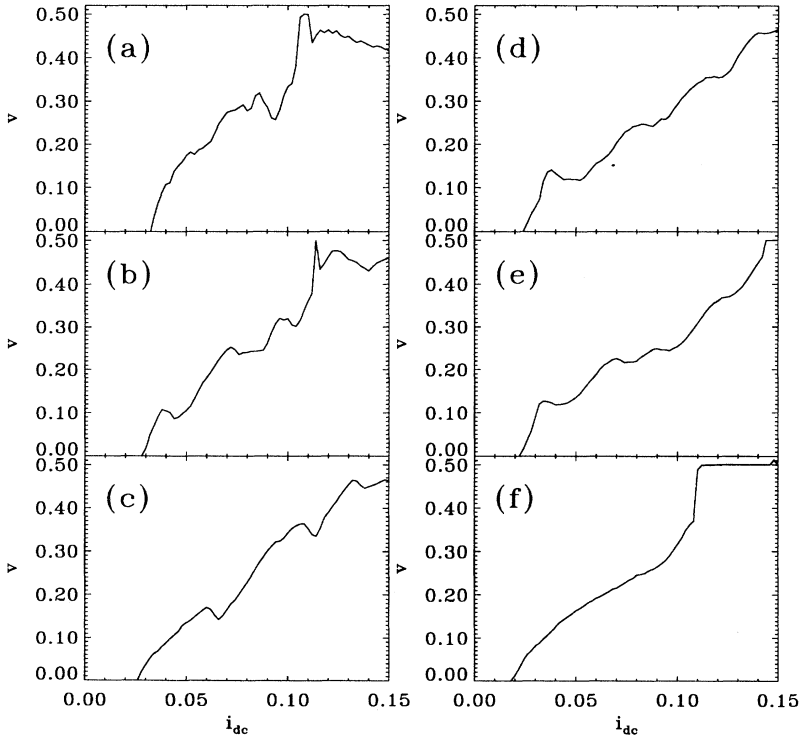

FIG. 14. IV characteristics in the turbulent phase for different couplings σ. For $\tilde{g} = 0.2$, $\Omega_{rf} = 0.8$, $i_{rf} = 0.61$. (a) $\sigma = 0.1$. (b) $\sigma = 0.2$. (c) $\sigma = 0.3$. (d) $\sigma = 0.4$. (e) $\sigma = 0.5$. (f) $\sigma = 0.8$.

VI. THERMAL NOISE EFFECTS

In this section we want to consider the effects of thermal noise on the turbulent phase for two reasons: (a) The thermal effects cannot be ignored in real experiments (then we must know if the phenomena studied in the previous sections are stable at finite temperatures); (b) the addition of noise in the dynamics of GCM's has shown interesting effects in previous studies,[18,19] correlated with the breakdown of the law of large numbers.

We consider the effect of temperature in the dynamical equations of the JJSA by adding the contribution of a Johnson noise in the shunt resistances of each junction, as it is common in the literature.[30] We also add a Johnson noise contribution in the resistive load. Therefore the dynamical equations are now given by

$$\ddot{\phi}_k + g\dot{\phi}_k + \sin\phi_k + (2\tilde{T}g)^{1/2}\eta_k(\tau) + i_L = i_{\rm dc} + i_{\rm rf}\sin(\Omega_{\rm rf}\tau)\ , \quad (16)$$

$$i_L = \frac{\sigma}{N}\sum_{j=1}^{N} g\dot{\phi}_j + \left(\frac{2\tilde{T}g\sigma}{N}\right)^{1/2}\eta_L(\tau)\ . \quad (17)$$

The thermal Johnson noise is given by the white noise terms $\eta_k(\tau), \eta_L(\tau)$, such that $\langle\eta_k(\tau)\rangle = 0$, $\langle\eta_k(\tau)\eta_{k'}(\tau')\rangle = \delta(\tau-\tau')\delta_{k,k'}$. Temperature is normalized such that $\tilde{T} = 2ekT/\hbar I_c$. We have done numerical simulations of these equations using a second-order Runge Kutta method suitable for stochastic differential equations,[36] and the same integration times and time steps as for the previous $\tilde{T} = 0$ calculations.

Let us study the effect of temperature on the breakdown of the law of large numbers. In Fig. 15 we show S_0 as a function of N for $\sigma = 0.4$ and for $i_{\rm dc} = 0.124$ (which corresponds to the turbulent regime) for different temperatures. We see that for $\tilde{T} = 0$, S_0 saturates for large N (breakdown of the law of large numbers). This effect is stable for small temperatures, and only after a critical $\tilde{T}_{c1} \approx 4\times10^{-5}$ is there a crossover to a $1/N$ behavior. Similar phenomena has been found when adding a white noise term to GCM's,[18] where also the $1/N$ behavior is recovered after a critical value of noise intensity.

More interesting, from the experimental point of view, is the behavior of S_0 as a function of temperature for a fixed large number of junctions (if N_* is the typical N for saturation of S_0 at $\tilde{T} = 0$, we consider $N > N_*$). In Fig. 16 we show the results for bias $i_{\rm dc} = 0.124$, $\sigma = 0.4$, and $N = 16384$ junctions. We find three different thermal regimes.

(i) For $\tilde{T} < \tilde{T}_{c1} \approx 4\times10^{-5}$, the broad-band noise *decreases* when increasing the temperature. This counterintuitive behavior is a consequence of the fact that there is a breakdown of the law of large numbers at $\tilde{T} = 0$. The addition of thermal noise reduces in part the subtle coherence that made S_0 saturate for large N. In other words, N_* increases when increasing the temperature. This leads to a decrease of S_0 when increasing $\tilde{T}$ at fixed N. Since there is still a breakdown of the law of large numbers, this is the temperature regime where the *turbulence* and the global coupling of the JJSA's are manifested.

(ii) For $\tilde{T}_{c1} < \tilde{T} < \tilde{T}_{c2}$, with $\tilde{T}_{c2} \approx 5\times10^{-3}$, S_0 remains *constant*. Now the $1/N$ law is fulfilled. Here the ϕ_j act as independent chaotic variables. In this temperature regime, the subtle coherence of the global coupling has been destroyed, and S_0 is mainly due to the *chaos* of the individual junctions.

(iii) For $\tilde{T} > \tilde{T}_{c2}$, S_0 *increases* with temperature. In this part the dynamics of the junctions is dominated by the thermal fluctuations, and therefore the broad-band noise S_0 is a consequence of the *thermal noise*.

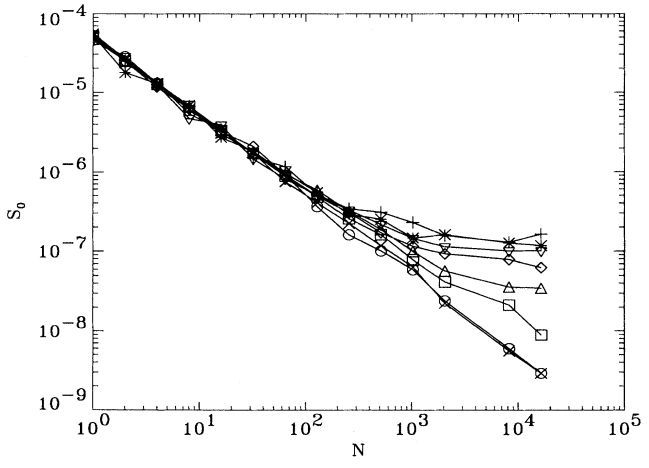

FIG. 15. Low-frequency limit of the power spectrum, $S_0 = \lim_{\omega\to0} S(\omega)$, as a function of the size of the array N. For $\tilde{g} = 0.2$, $\Omega_{\rm rf} = 0.8$, $i_{\rm rf} = 0.61$, $i_{\rm dc} = 0.124$, $\sigma = 0.4$, and different temperatures $\tilde{T}$: +, $\tilde{T} = 0$; $*$, $\tilde{T} = 1\times10^{-6}$; $\bigtriangledown$, $\tilde{T} = 2\times10^{-6}$; $\diamond$, $\tilde{T} = 5\times10^{-6}$; $\bigtriangleup$, $\tilde{T} = 1\times10^{-5}$; $\square$, $\tilde{T} = 2\times10^{-5}$; $\times$, $\tilde{T} = 5\times10^{-5}$; $\bigcirc$, $\tilde{T} = 1\times10^{-4}$.

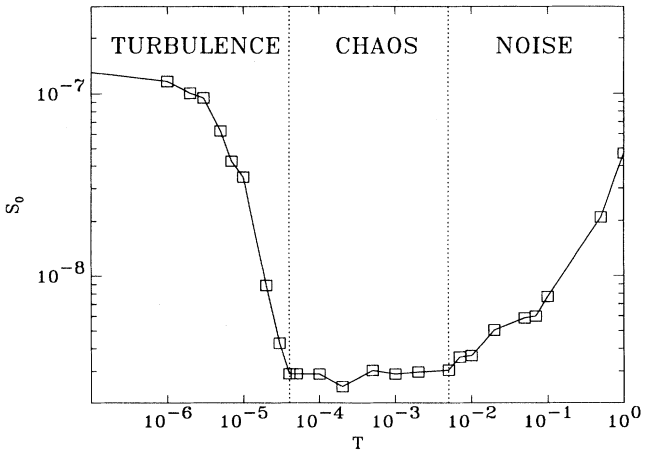

FIG. 16. Low-frequency limit of the power spectrum, $S_0 = \lim_{\omega\to0} S(\omega)$, as a function of the temperature $\tilde{T}$. For $\tilde{g} = 0.2$, $\Omega_{\rm rf} = 0.8$, $i_{\rm rf} = 0.61$, $i_{\rm dc} = 0.124$, $\sigma = 0.4$, for a large array, $N = 16384$.

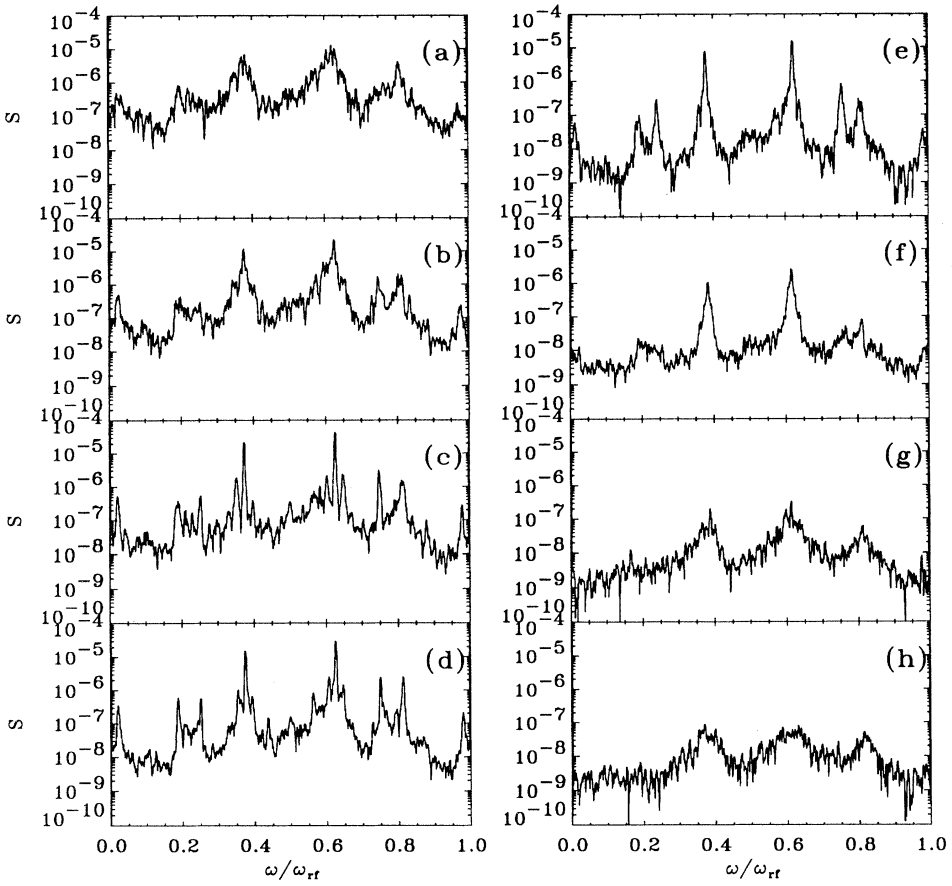

FIG. 17. Power spectrum for different temperatures. For $\tilde{g} = 0.2$, $\Omega_{rf} = 0.8$, $i_{rf} = 0.61$, $i_{dc} = 0.124$, $\sigma = 0.4$, $N = 16\,384$. (a) $\tilde{T} = 0$. (b) $\tilde{T} = 2\times10^{-6}$. (c) $\tilde{T} = 5\times10^{-6}$. (d) $\tilde{T} = 1\times10^{-5}$. (e) $\tilde{T} = 2\times10^{-5}$. (f) $\tilde{T} = 3\times10^{-5}$. (g) $\tilde{T} = 2\times10^{-4}$. (h) $\tilde{T} = 5\times10^{-4}$.

The thermal noise affects the full power spectrum in a surprising way. Perez *et al.*[19] found that in GCM's the broad peaks in the power spectrum sharpen up when increasing the noise. In Fig. 17 we show the power spectrum for $\sigma = 0.4$, $i_{dc} = 0.124$ as a function of temperature. We see that also in this case the broad peaks, due to the breakdown of the law of large numbers at $\tilde{T} = 0$, get sharper and better defined when increasing temperature [Figs. 17(a)–17(f)]. Only after $\tilde{T} > \tilde{T}_{c1}$ does the power spectrum start to become broadened by the thermal fluctuations [Figs. 17(g), 17(h)]. More quantitatively, following Ref. 19, we have defined the measure of sharpness,

$$W = -\log_{10}\left[\frac{1}{M}\frac{\sum_{l=1}^{M}\sum_{m=1}^{M}S(\omega_{l+m})S(\omega_m)}{\sum_{l=1}^{M}S(\omega_l)^2}\right], \quad (18)$$

where M is the number of discrete points in the spectrum. For a completely flat spectrum $W = 0$, and for a set of δ peaks, $W \to \infty$. We show in Fig. 18 the sharpness W as a function of $\tilde{T}$. We see that W increases with temperature until it reaches $\tilde{T}_{c1}$ where it drops abruptly.

Finally we analyze the effect of temperature in the pseudosteps in the IV characteristics. We show in Fig. 19 the IV curves for $\sigma = 0.4$ in the turbulent phase for different temperatures. We see that the pseudostep structure is stable up to temperatures much larger than $\tilde{T}_{c1}$ and slightly below $\tilde{T}_{c2}$, above which they disappear. Therefore, the pseudosteps seem to be more stable against thermal noise than the breakdown of the law of large numbers. This result suggests that even when both phenomena coexist, they are not completely correlated.

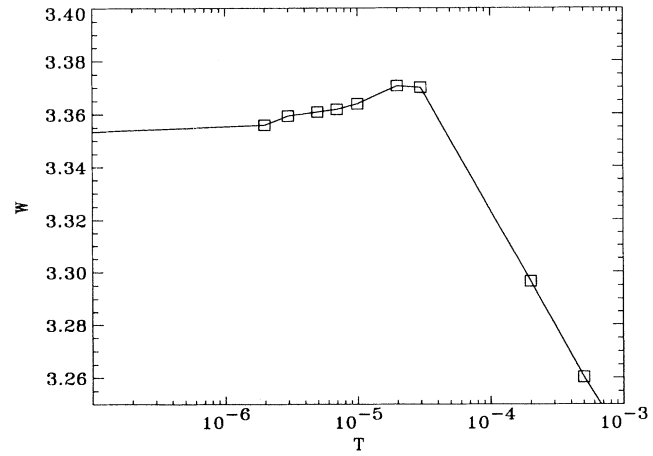

FIG. 18. Measure W of the sharpness of the peaks in the power spectra as a function of the temperature $\tilde{T}$. For $\tilde{g} = 0.2$, $\Omega_{rf} = 0.8$, $i_{rf} = 0.61$, $i_{dc} = 0.124$, $\sigma = 0.4$, and $N = 16\,384$.

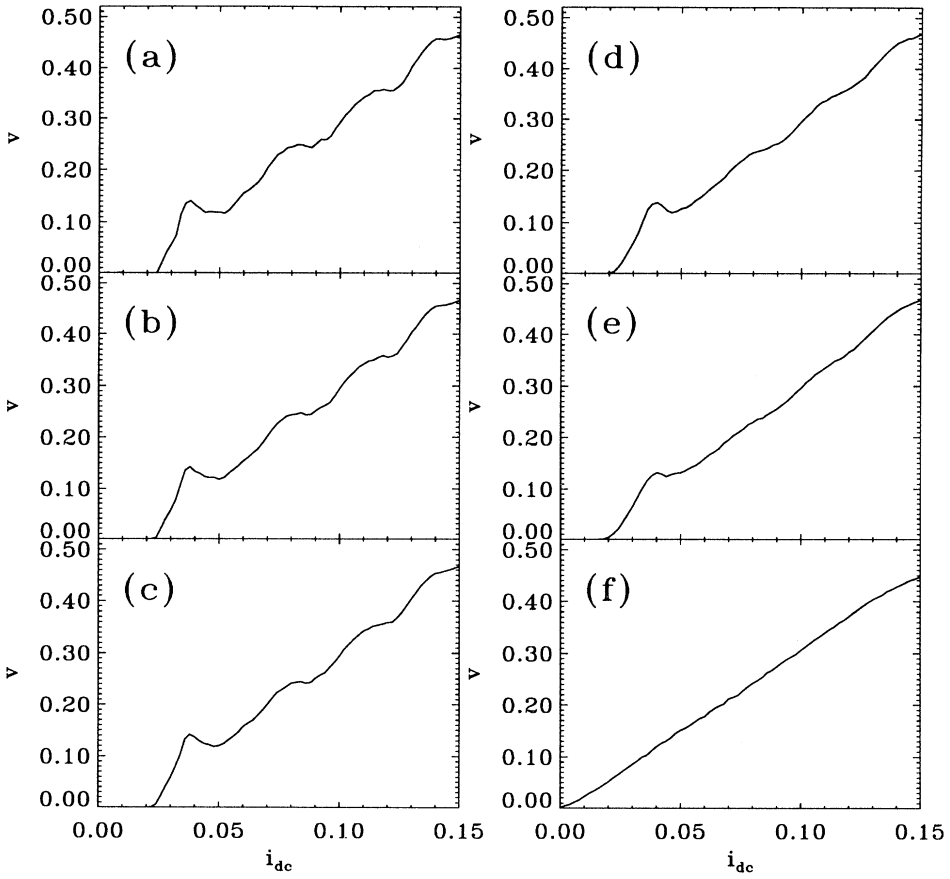

FIG. 19. *IV* characteristics in the turbulent phase for different temperatures $\tilde{T}$ and coupling $\sigma = 0.4$. For $\tilde{g} = 0.2$, $\Omega_{rf} = 0.8$, $i_{rf} = 0.61$. (a) $\tilde{T} = 0$. (b) $\tilde{T} = 1 \times 10^{-4}$. (c) $\tilde{T} = 2 \times 10^{-4}$. (d) $\tilde{T} = 5 \times 10^{-4}$. (e) $\tilde{T} = 1 \times 10^{-3}$. (f) $\tilde{T} = 1 \times 10^{-2}$.

VII. CONCLUSIONS

We have presented a system[11,12] in which many interesting phenomena that are being currently studied in globally coupled logistic maps[16–24] can be measured in concrete experiments. The JJSA's can show coherent, ordered, partially ordered, quasiperiodic, and turbulent phases in their *IV* characteristics. The coherent phase exists for $i_{dc} < i_c$ or for large bias currents. The ordered phase corresponds to the Shapiro steps, for which we have found that the number of big clusters is equal to the order of the step. The turbulent phase of the JJSA shows a breakdown of the law of large numbers. The new feature in this system is that this effect coexists with the appearance of pseudosteps in the *IV* characteristics.

A closely related system is charge density waves. Also in this case there are many coupled degrees of freedom, which have been recently described with a global coupling model.[37] Including a second time derivative term in their equations (due to the displacement current) may lead to the same kind of phenomena studied here.

Josephson junction series arrays like the one discussed in this paper can be fabricated with the present techniques.[13] One possible experiment consists in making an underdamped JJSA with a large number of junctions ($N \sim 10^3$–10^5). At very low temperatures, there will be true Shapiro steps, with no broad-band noise ($S_0 = 0$), and pseudosteps with broad-band noise ($S_0 \neq 0$). A measurement of the broad-band noise S_0 as a function of temperature should show first a plateau below a temperature T_{c2}, and then a sharp increase when decreasing temperature below a critical T_{c1} (for junctions with $I_c = 1$ μA, $T_{c1} \sim 1$ mK, $T_{c2} \sim 0.1$ K). This would be a clear indication of the breakdown of the law of large numbers. Of course, experiments with JJSA's with different number of junctions of the same characteristics will be a more direct verification. A comparison of the different *IV* curves and the different power spectra as a function of N would show clearly the breakdown of the law of large numbers and the emergence of pseudosteps, as described here.

ACKNOWLEDGMENTS

We acknowledge C. Pando-Lambruschini and G. Pérez for useful discussions. H.A.C. also acknowledges support from the Instituto Nazionale di Fisica Nucleare (Italy).

[1] See, for example, *KT Transition and Superconducting Arrays*, Proceedings of the 2nd CTP Workshop on Statistical Physics, edited by D. Kim *et al.* (Min Eum Sa, Seoul, 1993).
[2] P. Hadley and M. R. Beasley, Appl. Phys. Lett. **50**, 621 (1987); P. Hadley, M. R. Beasley, and K. Wiesenfeld, Phys. Rev. B **38**, 8712 (1988).
[3] K. Wiesenfeld and P. Hadley, Phys. Rev. Lett. **62**, 1335 (1989).
[4] K. Y. Tsang, S. H. Strogatz, and K. Wiesenfeld, Phys. Rev. Lett. **66**, 1094 (1991); K. Y. Tsang and I. B. Schwartz, *ibid.* **68**, 2265 (1992).
[5] S. E. Strogatz and R. E. Mirollo, Phys. Rev. E **47**, 220 (1993); S. Watanabe and S. E. Strogatz, Phys. Rev. Lett. **70**, 2391 (1993); Physica D **74**, 197 (1994).
[6] S. P. Benz, M. S. Rzchowski, M. Tinkham, and C. J. Lobb, Phys. Rev. Lett. **64**, 693 (1990); H. C. Lee, R. S. Newrock, D. B. Mast, S. E. Hebboul, J. C. Garland, and C. J. Lobb, Phys. Rev. B **44**, 921 (1991); S. E. Hebboul and J. C. Garland, *ibid.* **43**, 13 703 (1991).
[7] K. H. Lee, D. Stroud, and J. S. Chung, Phys. Rev. Lett. **64**, 692 (1990); J. U. Free, S. P. Benz, M. S. Rzchowski, M. Tinkham, C. J. Lobb, and M. Octavio, Phys. Rev. B **41**, 7267 (1990); M. Kvale and S. E. Hebboul, *ibid.* **43**, 3720 (1991); H. Eikmans and J. E. van Himbergen, *ibid.* **44**, 6937 (1991).
[8] D. Domínguez, J. V. José, A. Karma, and C. Wiecko, Phys. Rev. Lett. **67**, 2367 (1991); D. Domínguez and J. V. José, *ibid.* **69**, 414 (1992); Phys. Rev. B **48**, 13 717 (1993); Int. J. Mod. Phys. B **8**, 3749 (1994).
[9] F. Falo, A. R. Bishop, and P. S. Lomdahl, Phys. Rev. B **41**, 10 983 (1990); N. Gronbech-Jensen, F. Falo, A. R. Bishop, and P. S. Lomdahl, *ibid.* **46**, 11 149 (1992); R. Mehrotra and S. R. Shenoy, Europhys. Lett. **9**, 11 (1989); Phys. Rev. B **46**, 1088 (1992).
[10] R. Bhagavatula, C. Ebner, and C. Jayaprakash, Phys. Rev. B **45**, 4774 (1992).
[11] D. Domínguez and H. A. Cerdeira, Phys. Rev. Lett. **71**, 3359 (1993); in *Chaos in Mesoscopic Systems*, Proceedings of the Adriatico Research Conference, Trieste, 1993, edited by H. A. Cerdeira and G. Casati (World Scientific, Singapore, 1995).
[12] D. Domínguez and H. A. Cerdeira, Phys. Lett. A **200**, 43 (1995); in Proceedings of the ICTP-NATO Workshop, *Quantum Dynamics of Submicron Structures*, Trieste, edited by H. A. Cerdeira, B. Kramer, and G. Schön (Kluwer Academic, Dordrecht, 1995).
[13] A. K. Jain, K. K. Likharev, J. E. Lukens, and J. E. Sauvageau, Phys. Rep. **109**, 310 (1984); R. L. Kautz, C. A. Hamilton, and F. L. Lloyd, IEEE Trans. Magn. **MAG-23**, 883 (1987).
[14] S. P. Benz and C. J. Burroughs, Appl. Phys. Lett. **58**, 2162 (1991).
[15] J. P. Crutchfield and K. Kaneko, in *Directions in Chaos*, edited by Hao Bai-Lin (World Scientific, Singapore, 1987), p. 272.
[16] K. Kaneko, Phys. Rev. Lett. **63**, 219 (1989); Physica D **41**, 137 (1990); J. Phys. A **24**, 2107 (1991).
[17] K. Kaneko, Physica D **54**, 5 (1992).
[18] K. Kaneko, Phys. Rev. Lett. **65**, 1391 (1991); Physica D **55**, 368 (1992).
[19] G. Perez, S. Sinha, and H. A. Cerdeira, Physica D **63**, 341 (1993).
[20] G. Perez and H. A. Cerdeira, Phys. Rev. A **46**, 4792 (1992); G. Perez, C. Pando-Lambruschini, S. Sinha, and H. A. Cerdeira, *ibid.* **45**, 5469 (1992); S. Sinha, D. Biswas, M. Azam, and S. Lawande, *ibid.* **46**, 3193 (1992); **46**, 6242 (1992).
[21] S. Sinha, Phys. Rev. Lett. **69**, 3306 (1992).
[22] M. Ding and L. T. Wille, Phys. Rev. E **48**, R1605 (1993).
[23] A. S. Pinkovsky and J. Kurths, Phys. Rev. Lett. **72**, 1614 (1994).
[24] K. Kaneko (unpublished).
[25] B. A. Huberman, J. P. Crutchfield, and N. H. Packard, Appl. Phys. Lett. **37**, 750 (1980); E. Ben-Jacob, I. Goldhirsh, Y. Imry, and S. Fishman, Phys. Rev. Lett. **49**, 1599 (1982).
[26] M. H. Jensen, P. Bak, and T. Bohr, Phys. Rev. A **30**, 1960 (1984); **30**, 1970 (1984).
[27] M. Octavio and C. Readi Nasser, Phys. Rev. B **30**, 1586 (1984); M. Iansit, Q. Hu, R. M. Westervelt, and M. Tinkham, Phys. Rev. Lett. **55**, 746 (1985).
[28] R. L. Kautz and R. Monaco, J. Appl. Phys. **57**, 875 (1985); M. Levi, Phys. Rev. A **37**, 927 (1988).
[29] D. E. McCumber, J. Appl. Phys. **39**, 3113 (1968); W. C. Stewart, Appl. Phys. Lett. **10**, 277 (1968).
[30] A. Barone and G. Paternó, *Physics and Applications of the Josephson Effect* (Wiley, New York, 1982).
[31] S. Shapiro, Phys. Rev. Lett. **11**, 80 (1963).
[32] Recently, in Ref. 5, it has been shown that JJSA's with a resistive load, but overdamped ($g = \infty$), and with a dc drive ($I_{\rm rf} = 0$), have $N - 3$ constants of motion.
[33] D. Hansel, G. Mato, and C. Meunier, Phys, Rev. E **48**, 3470 (1993).
[34] K. Okuda, Physica D **63**, 424 (1993).
[35] D. Hansel and H. Sompolinsky, Phys. Rev. Lett. **68**, 718 (1992); Softky *et al.*, J. Neurosci. **48**, 1302 (1993); Wei Wang, G. Pérez, and H. A. Cerdeira, Phys. Rev. E **47**, 2893 (1993).
[36] H. S. Greenside and E. Helfand, Bell. Syst. Tech. J. **60**, 1927 (1981).
[37] J. Levy, M. S. Sherwin, F. F. Abraham, and K. Wiesenfeld, Phys. Rev. Lett. **68**, 2968 (1992); M. J. Higgins, A. A. Middleton, and S. Bhattacharya, *ibid.* **70**, 3784 (1993); A. Montakhab, J. M. Carlson, and J. Levy (unpublished).